Title

The conundrum of subspecies: morphological diversity among desert populations of the California vole (Microtus californicus, Cricetidae)

Journal

Journal of Mammalogy, 98(4)

ISSN

0022-2372

Authors

Patton, James L
Conroy, Christopher J

Publication Date

2017-08-01

DOI

10.1093/jmammal/gyx074

Peer reviewed

Journal of Mammalogy, 98(4):1010–1026, 2017
DOI:10.1093/jmammal/gyx074

The conundrum of subspecies: morphological diversity among desert populations of the California vole (*Microtus californicus*, Cricetidae)

James L. Patton* and Christopher J. Conroy

Museum of Vertebrate Zoology, University of California, 3101 Valley Life Sciences Building, Berkeley, CA 94720, USA (JLP, CJC)
Department of Integrative Biology, University of California, Berkeley, CA 94720, USA (JLP)

* *Correspondent: patton@berkeley.edu*

We examined geographic trends in 4 morphological data sets (both craniodental and colorimetric measurements and scores of cranial foramina and qualitative craniodental variables) within and among 5 subspecies of the California vole, *Microtus californicus*, that occur within or adjacent to the Mojave Desert in eastern California. These analyses are corollary to those previously published on the same samples using both mitochondrial and nuclear gene sequences and microsatellite loci. The morphological and molecular data sets are generally concordant in supporting the existing infraspecific taxonomy, although important conflicts are evident. With the combination of data sets, we are able to assign previously unknown samples to these infraspecific taxa. We define and provide an emended diagnosis of each subspecies using the criteria established by Willi Hennig in his 1966 assessment of the qualities and characteristics of infraspecific taxa, which he understood to be fundamentally different than the hierarchical phylogenetic system he established as the conceptual framework for taxa at the species level and above. Hennig's views are contrary to how the subspecies concept has been applied in much of recent mammalian taxonomy.

Key words: colorimetrics, *Microtus californicus*, Mojave Desert, morphometrics, qualitative characters, subspecies, taxonomy

California voles (*Microtus californicus*) occur predominantly in coastal and interior annual and perennial grasslands from northern Baja California through California west of the crest of the Sierra Nevada to southern Oregon. Populations also extend into saltwater marshes along the Pacific coast, riparian corridors coursing the low- to mid-elevation slopes of the Peninsular, Transverse, and Sierra Nevada ranges, and into the Mojave Desert in eastern California at springs and stream courses east of the Sierra Nevada, including the Owens, Mojave, and Amargosa river basins. Specimens identified as *M. californicus* from Early Holocene to Glacial age deposits (7.5 to 20.5 kya) are known from a handful of localities in the Mojave Desert of California and east as far as Tule Springs in Clark County, Nevada (FaunMap; http://www.ucmp.berkeley.edu/faunmap/). The species clearly had a wider range during the most recent cool and wet period (Wisconsinan) through this desert region than it does today.

Kellogg (1918) last reviewed the systematics of the California vole throughout its range, diagnosing 10 subspecies, 6 of which he named (see also Kellogg 1922). Seven additional infraspecific taxa were described in subsequent decades, bringing the total to 17 subspecies currently recognized or listed in taxonomic compendia (Hall 1981; Musser and Carleton 2005). Of these, 3 subspecies are restricted to the desert floor in eastern California and 2 others to montane areas at the adjacent southern and western margins of the Mojave Desert. One of these (*M. c. scirpensis*) is federally listed as Endangered; 2 are currently state listed as a Species of Special Concern (*M. c. mohavensis* and *M. c. vallicola*).

Conroy et al. (2016), using a combination of mitochondrial and nuclear gene sequences and microsatellite loci, confirmed the presence in the Mojave Desert of both the Northern and Southern species-wide mitochondrial clades identified previously (Conroy and Neuwald 2008). Southern Sierra Nevada and Owens Valley samples belong to the Northern mtDNA clade; Transverse Range, Mojave Desert floor, and Amargosa drainage samples are part of the Southern mtDNA clade. Each of these clades is further subdivided into more localized but well-supported lineages largely concordant in sample membership with analyses of microsatellite loci (Fig. 1). Microsatellite data

divide all population samples into 3 geographic units of equal strength: Owens Valley and southern Sierra Nevada samples; Transverse Range (San Gabriel and San Bernardino mountains) and adjacent Mojave Desert floor; and an isolated population in the Amargosa drainage. The 2 Northern mtDNA microsatellite groups abut one another at a point (Owens Lake) where most of the sample possesses intermediate genotypes (arrow; Fig. 1). The Southern mtDNA clade also divides into 2 microsatellite units that are geographically divisible into the 2 major mountain masses of the Transverse Range: the western San Gabriel Mts. plus those on the adjacent Mojave Desert floor, and the eastern San Bernardino Mts., again including samples on the adjacent Mojave Desert floor. The sample from the Amargosa drainage in the eastern Mojave Desert forms a microsatellite assemblage equal in its distinctness to that of northern and southern samples.

Conroy et al. (2016) did not address the status of the molecular clades they delineated in the context of Kellogg's taxonomy. Here, we examine patterns of geographic variation in morphological characters within and among populations of the California vole from the Mojave Desert to ascertain the ability of morphology alone to circumscribe the same genealogical units defined molecularly. Recent surveys and unreported specimens heretofore hidden in museum collections extend the range of this species in this area to 1) the Deep Springs and Saline valleys, small enclosed basins located east of the White and Inyo mountains that border the eastern side of the Owens Valley; 2) multiple localities along the desert base of the southern Sierra Nevada and Transverse Range (San Gabriel and San Bernardino mountains); and 3) onto the desert floor at China Lake Naval Air Weapons Station and Edwards Air Force Base (Fig. 2). We compare these samples to those of the 5 currently recognized subspecies from eastern California, namely *M. c. kernensis* Kellogg from the Kern River Plateau and adjacent Walker Basin and Piute Mts. at the southern terminus of the Sierra Nevada, *M. c. sanctidiegi* Kellogg from the conifer forests of the San Gabriel and San Bernardino mountains, *M. c. mohavensis* Kellogg from the upper Mojave River at Victorville, *M. c. scirpensis* Bailey from the Amargosa River southeast of Death Valley, and *M. c. vallicola* Bailey from the Owens Valley east of the Sierra Nevada. We use a combination of external and craniodental morphometrics, frequency variation in cranial foramina and qualitative craniodental traits, and colorimetric coefficients that define the dorsal pelage. These analyses emphasize the distinctness of each recognized subspecies and provide clear evidence for the allocation of our recently obtained samples to the subspecies as currently recognized. The groups identified are largely concordant with phylogeographic units previously identified by mitochondrial and nuclear DNA markers (Conroy et al. 2016; see presentation and

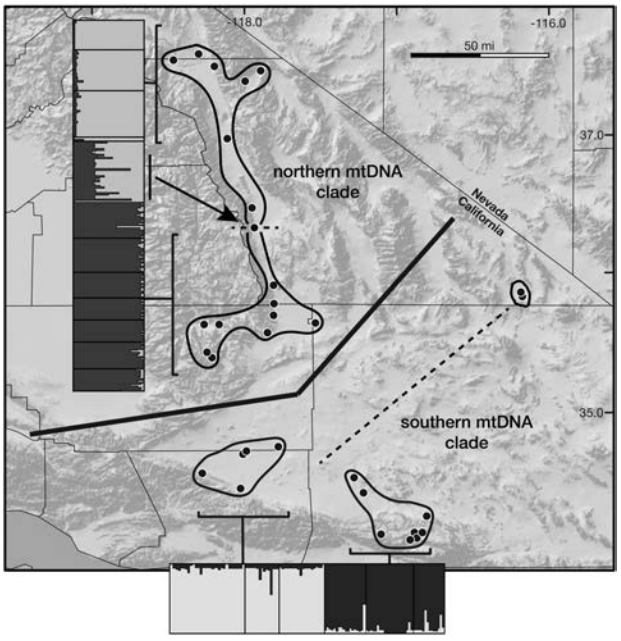

Fig. 1.—Molecular relationships among desert populations of the California vole (*Microtus californicus*): the heavy black line delimits the boundary separation between the Northern and Southern mtDNA clades defined by Conroy and Neuwald (2008); lighter black lines group population samples identified by a STRUCTURE posterior probability analysis based on nuclear microsatellite loci (see Conroy et al. 2016). The arrow and dashed line separating the Northern mtDNA clade members identify the intermediate sample from Owens Lake (OL); the dashed line linking the isolated eastern Mojave-Amargosa drainage sample signifies its membership as part of the Southern mtDNA clade but a nuclear genome of equal distinctiveness to those of both Northern and Southern groups.

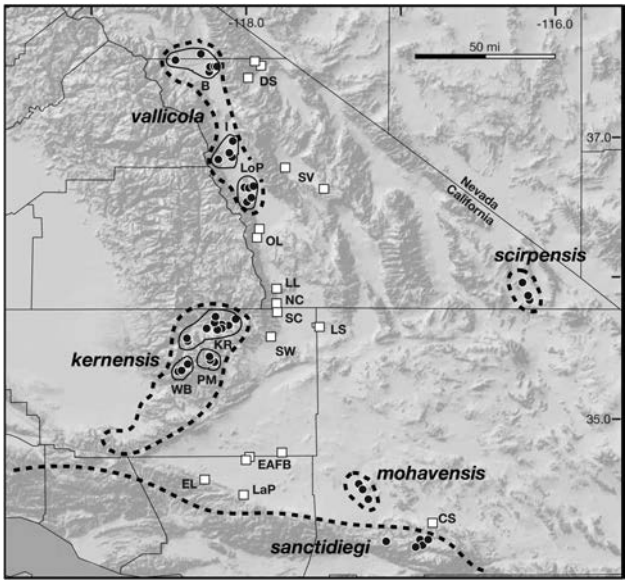

Fig. 2.—Localities of California voles (*Microtus californicus*) in the deserts of eastern California and adjacent mountain ranges. Black circles identify samples included in the analyses herein and grouped by currently recognized subspecies, the approximate ranges of which are circumscribed by heavy dashed ellipses (following Kellogg 1918). White boxes bordered by black identify samples from recently collected localities or historical sites that had not been included in previous studies. Geographic samples of the subspecies *kernensis* and *vallicola* used in the analyses are circumscribed by continuous black ellipses. All samples are labeled according to the list of localities in Table S1, Supplementary Data SD1.

discussion below) and thus reinforce the biogeographic hypothesis posited in that study.

We end by discussing the utility of the subspecies concept, which we define as a unit displaying strong concordance among geographically structured character sets, in mammalian systematics and conservation biology. We argue, however, that the current emphasis on molecular applications alone has incorrectly limited the definition of subspecies and thus the taxa that can and should be recognized.

Materials and Methods

Geographic samples.—Our samples belong to 5 subspecies of California voles whose ranges are either on the floor of the Mojave Desert (*mohavensis*, from the upper Mojave River at the northern base of the San Bernardino Mts.; *scirpensis*, from the Amargosa drainage southeast of Death Valley; and *vallicola*, limited to the floor of Owens Valley; Fig. 2) or in adjacent montane regions (*kernensis*, from the Kern River Plateau, Walker Basin, and Piute Mts. at the southern terminus of the Sierra Nevada; and *sanctidiegi*, broadly distributed in coastal southern California but, for our analysis, limited to the higher elevations of the San Bernardino Mts.). The allocation of our samples to these subspecies has a long history, extending to their original descriptions in the late 19th or early 20th centuries (Bailey 1898, 1900; Kellogg 1918, 1922) and continuing through successive faunal compendia (e.g., Grinnell 1933; Hall 1981:Map 454) to the present (Musser and Carleton 2005). There has been no review of these taxa, however, since Kellogg's nearly century-old treatise.

In addition to samples assignable to each subspecies are those from a number of newly discovered populations around the margins of the desert that partially fill the geographic gaps between the subspecies ranges as mapped by Kellogg (1918:figure 1) and Hall (1981:Map 454). These include specimens from the Deep Springs (DS) and Saline valleys (SV), both separated from the Owens Valley range of *vallicola* to the east by the intervening White-Inyo mountain axis. We also have 6 additional samples, including from the desert floor on China Lake Naval Air Weapons Station (Lark Seep, LS), from sites along the desert base of the southern Sierra Nevada in Indian Wells Valley (Soldier Wells at the mouth of Freeman Canyon, SW; Sand Canyon, SC; Ninemile Canyon, NC; and Little Lake, LL), and from Owens Lake (OL) at the southern end of Owens Valley. This set of samples fills the gap between the historic ranges of *kernensis* in the Kern River Plateau (KR) and Piute Mts. (PM and WB) and *vallicola* in the Owens Valley (Lone Pine, LoP; Independence, I; and Bishop, B). We also have 2 pooled samples from the northern base of the San Gabriel Mts. (Elizabeth Lake, EL; and Lake Palmdale, LaP) and adjacent desert floor on Edwards Air Force Base (EAFB) that are between the ranges of *kernensis*, *mohavensis*, and *sanctidiegi*; and a sample from Cushenbury Springs (CS), located on the desert floor at the northeastern base of the San Bernardino Mts., adjacent to the ranges of *mohavensis* and *sanctidiegi*. Our final sample is the federally listed as endangered *scirpensis* from the Amargosa drainage southeast of Death Valley, now restricted to the hot springs at Tecopa.

Our samples are primarily those in the Museum of Vertebrate Zoology (MVZ), supplemented by specimens from the National Museum of Natural History (USNM), the University of Michigan Museum of Zoology (UMMZ), the Cleveland Museum of Natural History (CMNH), and the Los Angeles County Museum of Natural History (LACM). Data are available from a total of 620 specimens from 72 individual localities (Fig. 2; pooled samples with included localities, georeferences, and samples sizes for each data set, as described immediately below, are listed in Supplementary Data SD1). No living animals were used in this study.

We examined character variation in 4 independent sets of morphological characters: 1) standard external and craniodental measurements, 2) dorsal pelage colorimetrics, 3) cranial foramina, and 4) qualitative craniodental traits, as detailed below.

External and craniodental morphometrics.—We obtained external measurements (total length [TOL], tail length [TAL], hind foot with claw length [HF], ear height from the notch [E], and body mass [MASS]) from specimen labels. We also took 16 craniodental measurements with digital calipers, at 0.01 mm precision, as follows: condyloincisive length (CIL—anterior margin of upper incisors to posterior margin of occipital condyles); nasal length (NL—midline length of nasal bones); nasal width (NW—width of nasals at their widest point); zygomatic breadth (ZB—greatest distance across the outside edges of the zygomatic arches); least interorbital distance (IOC—minimum distance across frontal bones between the orbits); interparietal width (IPW—transverse distance across interparietal bone); interparietal length (IPL—midline anterior-posterior length of the interparietal bone); length of bony palate (BPL—distance from posterior margin of upper incisors to anterior margin of mesopterygoid fossa); length of incisive foramina (IFL—distance from anterior to posterior margins of incisive foramina); mastoid breadth (MB—greatest distance across mastoid processes); maxillary toothrow length (MTRL—distance from anterior face of PM4 to posterior face of M3 taken at the alveolus); cranial depth (CD—vertical distance from ventral surface of bullae to the top of cranium); and mandibular length (ManL—length of mandible from posterior ventral margin of incisor alveolus to posterior margin of condyloid process). We measured separately the occlusal length of each left maxillary molar (L-M1, L-M2, and L-M3) using a calibrated micrometer with a Dino-Lite AD4113TL digital microscope (AnMo Electronics Corp., New Taipei City, Taiwan), at a precision of 0.001 mm. Data are available from 327 adult individuals (defined as specimens with a fused basioccipital-basisphenoid suture and non-rugose tympanic bullae) with undamaged skulls from 65 separate localities.

Colorimetric analyses.—We measured dorsal color reflectance with an X-Rite Digital Swatchbook spectrophotometer (X-Rite, Inc., Grandville, Michigan) on a total of 398 study skins of voles from 59 localities. We set the spectrophotometer to compare measured colors to the CIE (Commission Internationale de l'Éclairage, or International Commission on

Illumination) Standard Illuminant F7 for fluorescent illumination, which represents a broadband daylight fluorescent lamp (6,500 K). We chose this standard because all measurements were taken indoors under fluorescent ambient lighting. The instrument provides a reflectance spectrum (390–700 nm) of the object being measured as well as tri-stimulus color scores (CIE X, Y, and Z) that can be directly compared to the Munsell or other color references (Hill 1998). We used the mean of 5 separate measurements taken on the middorsal surface of the skin using a 3 mm port from specimens with adult, unworn, and nonoily pelage.

Cranial foramina.—Data are available from 272 specimens collected from 55 separate localities. We scored 7 foramina that are bilaterally present in the skulls of most mammals, as characterized by Berry and Searle (1963). The squamosal foramen (SqF) and maxillary foramen (MaxF) were either present or absent, on one or both sides, in all specimens. We scored each specimen as 1 if the foramen was absent or 3 if present on both sides of the skull; a value of 2 was given to bilaterally asymmetrical individuals. The frontal (FF), preorbital (PoF), hypoglossal (HypoF), and accessory mental foramina (AMF) were always present as a single or divided aperture. These were scored as 1 if singular or 2 if double on both sides. Finally, the major palatal foramina (MPF), located on the posterolingual margin of the palate, are always present as multiple openings; a score of 1 was given if a single, enlarged fenestra dominated, and a score of 3 if multiple fenestrae were approximately equal in size. Bilateral differences for all foramina were scored as 2 for left and right sides, respectively. AMF proved to be uniformly expressed as a single opening in all specimens we examined and was thus eliminated from further analysis. And both FF and PoF, while variable among individuals, exhibited no difference in their distribution among the 5 subspecies samples by χ^2 contingency tests; these were also excluded from our final analyses.

Craniodental qualitative traits.—Kellogg (1918) described several qualitative characteristics of the skull and maxillary teeth that he used in his diagnoses of the subspecies he recognized. We were able to score, with consistency and with reasonable objectivity, 9 traits in 533 specimens from 75 localities, as follows: 1) degree of procumbency (Fig. 3a), scored as 1 = orthodont (upper incisors not, or barely, visible when tip of rostrum is viewed from above) or 2 = proodont (upper incisors plainly visible from above); 2) extension of ascending premaxillary wings distal to termination of nasal bones (Fig. 3b), scored as 1 = short (extension < width of 1 nasal bone at distal margin) or 2 = long (extension > width of 1 nasal bone); 3) proximal shape of nasal bones (Fig. 3b), scored as 1 = parallel or weakly tapered or 2 = strongly tapered; 4) posterior margins of nasal bones (Fig. 3b), scored as 1 = squared or 2 = notched; 5) shape of incisive foramina (Fig. 3c), scored as 1 = oval, 2 = distally tapered, or 3 = distally expanded; 6) proportion of incisive foraminal opening occupied by bulbous premaxillary part of septum (Fig. 3c), scored as 1 = short (≤ ½ length of opening) or 2 = long (> ½ length of opening); 7) shape of posteroloph of M2 (Fig. 3d), scored as 1 = single loop present, or 2 = double loop present; 8) degree of development of 4th tine on the labial side of M3 (Fig. 3e), scored as 1 = not present, 2 = weakly present, or 3 = strongly present; and 9) indentation of labial side of posteroloph of M3 (Fig. 3e), scored as 1, no indentation present, 2 = weakly indented, or 3 = deeply indented. Each of these attributes was variable and differentially apportioned among the 5 subspecies samples; all were thus included in our analyses.

Statistical procedures.—For each data set, we first compared samples of the 5 subspecies that occur in the study area (Fig. 2; Table S1, Supplementary Data SD1). We wished to determine the degree to which each of these historically recognized taxa could be defined and diagnosed by the suite of characters we examined. Following confirmation (below) that each subspecies was, in fact, diagnosable, we then compared each sample from regions where California voles were heretofore unknown.

We obtained univariate summaries of craniodental and colorimetric variables and frequencies of foramen and qualitative character scores with JMP-Pro (version 12; SAS Institute Inc., Cary, North Carolina). We used JMP-Pro for multivariate principal components (PCA) and canonical variates analyses (CVA) for the continuous craniodental and colorimetric data and PAST3 (Hammer et al. 2001) for multivariate correspondence analysis (MCA) of the categorical scorings of foramina and qualitative craniodental character sets. All CVA were based on the 5 subspecies samples defined as a priori groups, following Kellogg (1918), with the 12 new and unaligned samples treated as "unknown." Craniodental variables were log-transformed after replacing 13 instances of missing variables from 4 individuals (SV sample) with the mean for their respective sample. PCA was performed to obtain PC-1 scores, a general multivariate expression of size, and we used CVA to obtain a reduced-axis perspective on overall craniodental differences among the defined groups. We examined colorimetric variables by CVA using the 3 raw tri-chromatic values obtained from each specimen. For the foramina data set, we first examined bilateral asymmetry by Spearman rank correlation of foramen score on both sides of the skull. As the correlation coefficient in each case was positive and highly significant (*Rho* ranged from 0.492 [z-value = 5.896] for MPF to 0.970 [z-value = 11.841] for the SqF, with $P < 0.0001$ for all comparisons), the 2 sides of the skull generally express the same condition. We thus combined the left and right scores for all specimens and used 2-way contingency tests to compare frequencies of each foramen among the 5 subspecies population samples. We then reduced these data to orthogonal components and factor scores by MCAs, a procedure similar to PCA but designed for categorical variables, using PAST3 (Hammer et al. 2001). We treated the set of 9 qualitative craniodental scores in the same fashion. Finally, for both categorical data sets we then performed a canonical analysis on their respective factor scores for all recovered axes. While unconventional, this last step was undertaken to obtain posterior probabilities of a priori group assignment for specimens of each "unknown" geographic sample comparable to those obtained by CVA for the 2 continuous data sets (see, for example, Jombart et al. 2010).

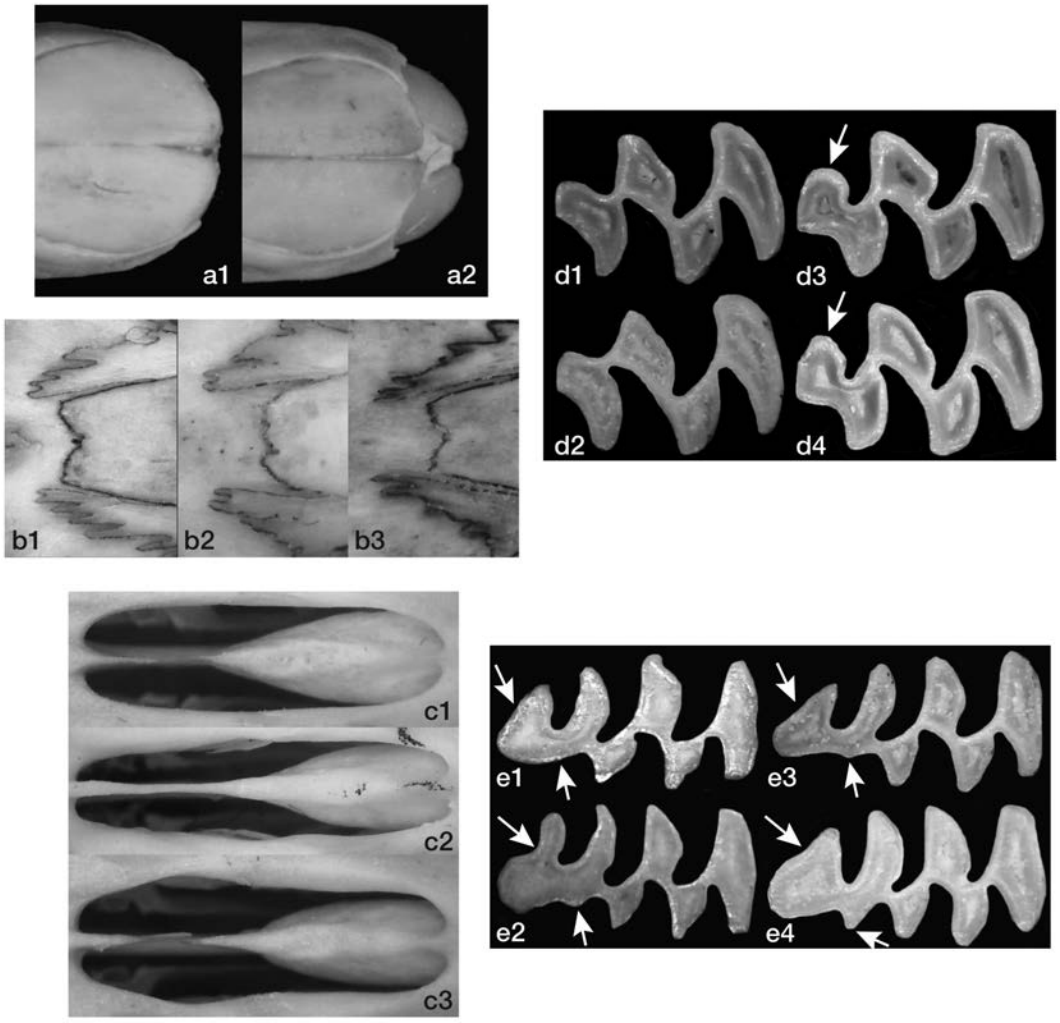

Fig. 3.—Qualitative craniodental characters: a—degree of procumbency (a1 = orthodont [score 1]; a2 = proodont [score 2]). b—length of ascending branches of premaxillae and shape of proximal margin of nasals (b1 = ascending branches short [score 1], nasals tapered [score 2], and notched [score 2]; b2 = ascending branches long [score 2], nasals parallel [score 1], and square [score 1]; b3 = ascending branches long [score 2], nasals tapered [score 2], and notched [score 2]). c—shape of incisive foramina and length of premaxillary part of septum (c1 = oval [score 1] and long [score 2]; c2 = tapered [score 2] and short [score 1]; c3 = expanded [score 3] and short [1]). d—internal lobe on posterior triangle of left M2 (d1 and d2 = absent [score 1]; d3 and d4 = present (arrows) [score 2]). e—4th tine on labial side and indentation on lingual side of posterior lobe of left M3, white arrows (e1 = no 4th tine [score 1] and no indentation [score 1]; e2 = weakly developed 4th tine [score 2] and deep indentation [score = 3]; e3 = weak 4th tine [score 2] and no indentation [score = 1]; e4 = strongly developed 4th tine [score 3] and shallow indentation [score 2]).

To determine if the 5 subspecies are diagnosably separate for each data set, we compared the respective PCA, CVA, or MCA scores for those axes where their eigenvalue was > 1.0 and where axis scores exhibited significant differences among them based on 1-way analysis of variance (ANOVA). We applied a Bonferroni correction for multiple comparisons between subspecies or individual sample pairs based on Tukey–Kramer post hoc tests. Since our samples of both *kernensis* and *vallicola* were distributed across relatively broad and ecologically heterogeneous ranges (Fig. 2), we first tested whether it was appropriate to pool each set of within-taxon samples prior to the 5 subspecies comparisons. Here, we divided each set of taxon samples into groups defined by geographic and ecological proximity and then examined scores derived by CVA, as above, by 1-way ANOVA and Tukey–Kramer post hoc tests. These analyses included 3 geographic groups of both *kernensis* (samples from the Kern River Plateau [KR; see Table S1, Supplementary Data SD1, including the holotype], those from Walker Basin [WB], and those from the Piute Mts. [PM]) and *vallicola* (those from the vicinity of Lone Pine [LoP, including specimens from the type series] at the southern end of the Owens Valley, from the vicinity of Independence [I] in the central Owens Valley, and those from near Bishop [B] at the northern end of the Owens Valley; Fig. 2). As these analyses confirmed the overall homogeneity of geographic samples of each subspecies (see below), we then used each historically defined set of samples for the 5 subspecies as a priori defined groups to which specimens from all other localities were then compared in a CVA, and used the posterior probabilities of group membership to assess the allocation of those samples to 1 or more of the defined subspecies. We also determined the concordance of group membership derived from each data set by contingency tests.

Results

Geographic differentiation within subspecies

Here, we assess the degree of geographic variation among each triad of samples of the subspecies *kernensis* and *vallicola* (Fig. 2), a necessary step to determine if all samples could be pooled for global analyses measuring the distinctness of all 5 currently recognized taxa from our study area. We report only summary comparisons for multivariate PCA, CVA, or MCA analyses across the 4 data sets, by 1-way ANOVA of the major axis scores (Tables S2.1 and S2.2, Supplementary Data SD2). Most multivariate data summaries exhibited no significant difference among the respective samples of either taxon; for those that did, *P*-values were generally only weakly significant ($P < 0.05$). CV-1 for the craniodental variables explained from 62% and 79% for *kernensis* and *vallicola*, respectively, of the total variance in the data, yet the scores on this axis did not differ significantly (1-way ANOVA, $P = 0.19$ for *kernensis* and $P = 0.95$ for *vallicola*). There was, however, slight differentiation in multivariate "size" (PC-1 scores) for both taxon samples ($P = 0.02$ for *kernensis*, with the WB samples marginally different from the other 2; $P = 0.03$ for *vallicola*, with the LoP sample separated, again marginally). CV-1 derived from the tri-chromatic color coefficients explained 99% of the variance in both subspecies samples; these scores were uniform among the samples of *kernensis* ($P = 0.92$) but in *vallicola* the northern Bishop sample (B) was marginally different from the 2 more southern samples ($P = 0.02$). Weak differentiation was present for foraminal MCA-1 scores for both taxa ($P = 0.03$ and $P = 0.03$, respectively), but not for scores of other MCA axes. MCA-1 explains 51% and 44% of the total variance in the respective analyses of *kernensis* and *vallicola*. Finally, the distribution of qualitative craniodental scores was uniform among the 3 samples of *kernensis* (MCA-1, $P = 0.12$; MCA-2, $P = 0.94$) but the *vallicola* samples exhibited differences on MCA-2 ($P = 0.01$), with those from Bishop contrasting slightly from the Independence ($P = 0.01$) and Lone Pine ($P = 0.001$) samples. This axis explained only 18% of the total variation for *vallicola*.

Overall, we judge that the geographic samples of both *kernensis* and *vallicola* were sufficiently homogeneous across all data sets to be combined in comparisons among the 5 currently recognized subspecies of California voles that lie within or border the Mojave Desert. The few pairwise sample differences noted were either only weakly differentiated or the particular multivariate summary explained only a small amount of the total variation expressed in the character set.

Uniqueness of the 5 desert subspecies

In the 5 subspecies multivariate analyses for each data set, 5 axes, alone or in combination among the data sets, explained at least 70% of the total pool of variation in each CVA (on raw variables for quantitative character sets or MCA scores for qualitative sets) and PCA analysis (Supplementary Data SD3): color CV-1 (85.6%; Table S3.1, Supplementary Data SD3), craniodental CV-1 (44.7%; Table S3.2) plus CV-2 (27.1%; Table S3.2, Supplementary Data SD3), foramina CV-1 (84.2%; Table S3.5, Supplementary Data SD3), and qualitative CV-1 (83.1%; Table S3.7, Supplementary Data SD3). PC-1 for the craniodental variables (Table S3.3, Supplementary Data SD3), included as an index of overall size, explained only 48% of the variation in that analysis. For these 6 axes, 49 of the 60 possible pairwise subspecies comparisons, based on Tukey–Kramer post hoc tests derived from 1-way ANOVAs, were highly significant *P* (< 0.001 to < 0.0001; Table S4.1, Supplementary Data SD4). Samples of *kernensis* differed from those of *vallicola* and *scirpensis* for all 6 analyses of the 4 character sets, as does *vallicola* relative to *mohavensis*. Samples of *vallicola* differed from those of *scirpensis* in 5 of the 6 analyses (83%) as did *scirpensis* relative to both *mohavensis* and *sanctidiegi*, and *mohavensis* in comparison to *sanctidiegi*. Only those comparisons between *kernensis* and both *mohavensis* (66%) and *sanctidiegi* (50%) or between *vallicola* and *sanctidiegi* (66%) lacked substantial differentiation. The levels of morphological character differentiation among these 5 currently recognized subspecies are depicted in Fig. 4. Note, however, that those paired subspecies samples with less than 80% diagnosability belong to different mtDNA clades, as *kernensis* and *vallicola* are members of the Northern mtDNA clade while *mohavensis* and *sanctidiegi* belong to the Southern clade (Fig. 1; see Conroy et al. 2016).

Classification matrices of specimens to subspecies in each of the separate canonical analyses, and thus in their ability to correctly assign specimens to subspecies, were strongly concordant. On average, between 62% and 77% of all specimens were correctly classified to their a priori defined subspecies across the 4 character data sets (see Table S4.2, Supplementary Data SD4). Contingency tests comparing these classification distributions were uniformly nonsignificant within each subspecies (χ^2 ranged from 32.766 to 45.408, *d.f.* from 30 to 33, and *P*-values from 0.07 to 0.39 across the 5 subspecies comparisons; Table S4.3, Supplementary Data SD4). Multiple, independent character sets thus documented substantial morphological diversity among, but concordance within, regional population units grouped by their current taxonomic arrangement as 5 subspecies.

Allocation of nonaligned samples

We assessed the allocation of specimens from localities not previously included in any prior morphological study by their posterior probability of assignment to each of the 5 subspecies samples delineated above based on the CVA analyses of each character set. For this, we performed separate analyses for those samples from the desert floor geographically adjacent to, and thus potentially offering connections between, the *kernensis–vallicola* and *mohavensis–sanctidiegi* taxon pairs. We judged separate analyses appropriate not only because of geographic proximity to each of these subspecies pairs but also because of unambiguous assignments of the majority of these samples derived from both mtDNA and microsatellite analyses (see Conroy et al. 2016).

Our 1st analysis included the western and northern cluster of samples in our study area—China Lake (LS), Indian Springs

Valley north to Owens Lake (SW, SC, NC, LL, and OL), and both Saline (SV) and Deep Springs (DS) valleys—relative to *kernensis* and *vallicola* (Fig. 2). Our 2nd analysis focused on those samples from the desert floor to the immediate north of the San Gabriel and San Bernardino mountains—Elizabeth Lake (EL), Lake Palmdale (LaP), Edwards Air Force Base (EAFB), and Cushenbury Springs (CS)—relative to *sanctidiegi* and *mohavensis*. For both sets of comparisons, we also included the single sample of *scirpensis*, far removed geographically yet hypothesized to have been derived historically via paleo-drainage connections from both Owens Lake to the Amargosa River system via the intervening China Lake and Panamint valleys and the separate connection between the Mojave River into the Amargosa River (summarized in Conroy et al. 2016).

Allocation of northern samples.—Samples of the 3 subspecies a priori groups were strongly differentiated from each another, and consistently so across all 4 character data sets (Table S5.1, Supplementary Data SD5). Posterior probabilities of within-taxon specimens ranged from a low of 0.6599 (foramina, *vallicola*) to a high 0.9997 (craniodental, *scirpensis*), and mean values for the combined data sets ranged from 0.7653 (*vallicola*) to 0.8286 (*kernensis*).

We summarize the allocation of individual specimens from each of the 8 nonaligned northern samples (DS, SV, OL, LL, NC, SC, SW, and LS) with respect to the 3 a priori defined subspecies in a ternary diagram depicting mean sample posterior probabilities from the CVA of each of the 4 individual character sets (Fig. 5).

Overall, the combined 6 separate multivariate summaries undertaken for the 4 data sets (scores for color CV-1, craniodental CV-1, CV-2, and PC-1, foramina CV-1, and craniodental qualitative CV-1) strongly and uniformly aligned samples from the southern end of Owens Lake (OL), Indian Wells Valley (SW, SC, NC, and LL), and China Lake (LS) with the geographically adjacent subspecies *kernensis*. The mean posterior probability of group assignment to *kernensis* was uniformly very high for each of these 6 samples (range 0.760 for OL to 0.897 for SW) and low to either *scirpensis* (range 0.042 [LL] to 0.093 [LS]) or *vallicola* (0.054 [SW] to 0.181 [NC]; Table S5.1, Supplementary Data SD5). Even with respect to the separate character sets, these samples exhibited little evidence of admixture with either *vallicola* to the north or *scirpensis* to the east. Probabilities of individual assignment to *kernensis* for the 4 data sets ranged from 67% (LS, color) to 96% (SW, craniodental). All other individual posterior probabilities were between 72% and 93% in their assignments to *kernensis*. Of the 327 specimen assignments summed across the 4 data sets, 293 (90.3%) were classified as *kernensis*; only 15 (4.7%) were classified as *scirpensis* and 19 (5.0%) as *vallicola* (Table S5.2, Supplementary Data SD5). Only the Owens Lake (OL) sample contained specimens with reasonable assignments as subspecies other than *kernensis*, with 10 individuals (13.9%) to *vallicola*, but even this sample was overwhelmingly classified as *kernensis* (58 of 72 specimens, or 80.6%). The concordance of individual posterior probabilities and thus classification assignment for all 4 data sets was remarkably strong.

The taxon linkages of the Saline Valley (SV) and Deep Springs Valley (DS) samples, however, were more complex, as each exhibited a more substantial degree of admixture with

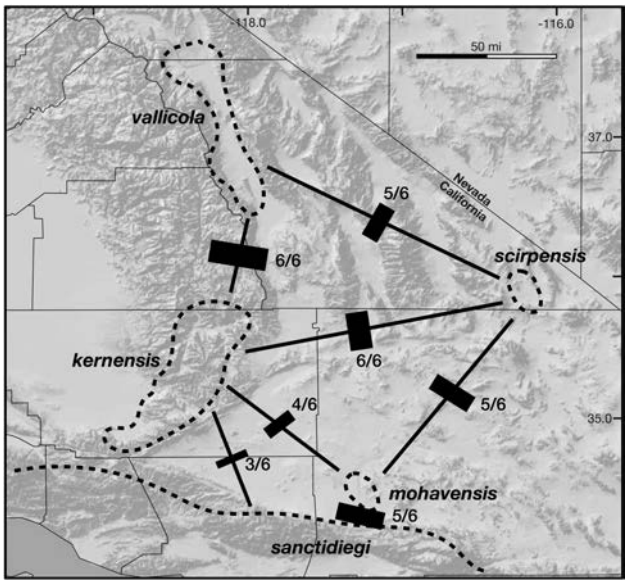

Fig. 4.—Character differentiation among geographically adjacent subspecies of the California vole (*Microtus californicus*) in the Mojave Desert floor and bordering montane regions of California. The width of the bars indicates the number of morphological character set analyses that are significantly different in each pairwise comparison.

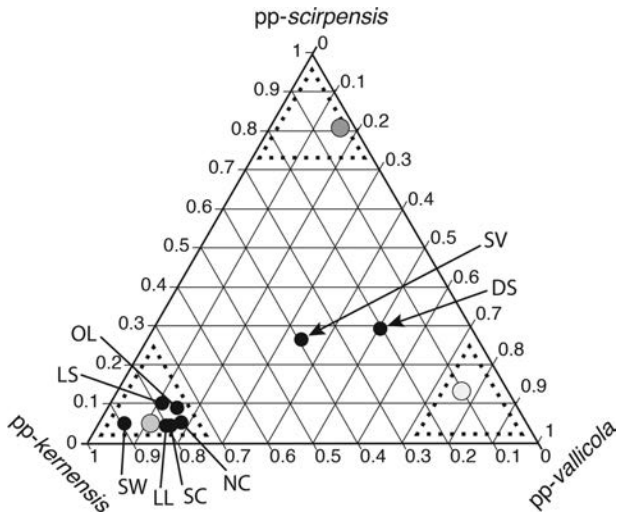

Fig. 5.—Mean sample posterior probabilities derived from canonical analyses of each of the 4 data sets for all northern samples of the California vole (*Microtus californicus*), with the 2 northern subspecies (*kernensis* and *vallicola*) plus *scirpensis* as a priori groups. The dotted triangles in each corner circumscribe the approximate 75% boundary for inclusion; the gray-filled circles represent the mean posterior probabilities for each of the 3 a priori subspecies (medium gray = *kernensis*; light gray = *vallicola*; dark gray = *scirpensis*); and the black circles are the mean posterior probabilities of group assignment for the 8 nonaligned localities, each identified by the locality acronym (DS = Deep Springs Valley; SV = Saline Valley; OL = Owens Lake; LL = Little Lake; NC = Ninemile Canyon; SC = Sand Canyon; SW = Soldier Wells; and LS = Lark Seep; see Fig. 2).

at least 2 subspecies samples (Fig. 5; Tables S5.1 and S5.2, Supplementary Data SD5). These 2 samples are an enigma with respect to both their physical isolation (each within enclosed basins separated by major habitat barriers to the other and to all other known areas inhabited by California voles) as well as their patterns of admixture relative to the 3 proximate subspecies. Character data sets for the Saline Valley samples were unique with respect to their discordant allocation to these subspecies and, as a result, to the general pattern of overall posterior probability of assignment. For example, the foramina data set strongly linked SV to *kernensis* (14 of 16 individuals, or 88%); both color and craniodental data supported a close tie with *vallicola*, albeit at a lower degree in both cases (respectively, 9 of 15 [60%] and 9 of 17 [53%]); yet qualitative craniodental characters were more similar to the distribution of these characters in *scirpensis* (10 of 16 [63%] of assignments; Table S5.2, Supplementary Data SD5). Thus, the average posterior probability of assignment to each of the 3 subspecies was relatively uniform: 0.349 to *vallicola*, 0.255 to *scirpensis*, and 0.395 to *kernensis* (Table S5.1, Supplementary Data SD5). This sample was remarkable for its apparent level of morphological admixture to all 3 a priori defined taxa, as reflected by its mean intermediate position in the ternary plot (Fig. 5).

Deep Springs Valley is about 19 km, direct line, east of Owens Valley but separated from the contiguous range of *vallicola* by Westgard Pass, the 2,225-m elevation, piñon-juniper-clothed low divide separating the White and Inyo mountains. It is about 225 km northwest of the known range of *scirpensis* in the Amargosa River drainage and 117 km north of the range of *kernensis* in the Kern River Plateau at the southern terminus of the Sierra Nevada. Perhaps unsurprisingly, therefore, this sample aligned most strongly with *vallicola* for all 4 data sets in both mean character posterior probabilities (0.506, Table S5.1, Supplementary Data SD5) and relatively high levels of assignment (from 59% [13 of 22 individuals for foramina] to 81% [17 of 21 individuals for qualitative craniodental], with color and craniodental mensural characters in between [62% to 67% assignment; Table S5.2, Supplementary Data SD5]). Only color suggested a reasonable connection to *kernensis* (6 of 21 specimen assignments, or 29%) but both craniodental and foraminal characters supported a connection with *scirpensis* (27% and 32%, respectively, of assignments). Overall, the mean posterior probabilities placed this sample, as with Saline Valley, in a rather intermediate position relative to "pure" members of each of the 3 subspecies in the ternary plot, but closest to *vallicola* (Fig. 5).

Allocation of southern samples.—Morphological distinction among these 3 subspecies samples (*mohavensis* from the Mojave River, *sanctidiegi* from the adjacent Transverse Range, and *scirpensis* from the Amargosa River) was also both sharp and consistent across the 4 character data sets (Table S6.1, Supplementary Data SD6). For the different character sets, mean posterior probabilities of group membership varied within subspecies from a low of 0.6602 (qualitative for *sanctidiegi*) to a high of 0.9999 (craniodental for both *sanctidiegi* and *scirpensis*). The overall mean posterior probability for each of the a priori taxon samples ranged from a minimum of 0.7664 (*sanctidiegi*) to a high of 0.9198 (*scirpensis*).

We again summarize the allocation of individual specimens from each of the 4 nonaligned southern samples (CS, EAFB, EL, and LaP) with respect to the 3 a priori defined subspecies in a ternary diagram depicting mean sample posterior probabilities from the CVA of each of the 4 individual character sets (Fig. 6).

Each of these 4 nonaligned samples from the base of the Transverse Range (EL, LaP, CS) and adjacent floor of the Mojave Desert (EAFB) were somewhat intermediate between *sanctidiegi*, which occupies the higher elevations of that range, and *mohavensis*, restricted to a narrow corridor along the adjacent Mojave River (Fig. 6; for locality geography, see Fig. 2). Mean posterior probabilities of assignment to *sanctidiegi* were relatively uniform for all 4 nonaligned samples, ranging from 0.5361 (EAFB) to 0.6645 (LaP). These samples tended toward *mohavensis* (Fig. 6), where posterior probabilities ranged from 0.2453 (LaP) to 0.3424 (EAFB), but they exhibited no connection to *scirpensis*, where mean posterior probabilities ranged only from 0.0902 (LaP) to 0.1363 (CS; Table S6.1, Supplementary Data SD6). Furthermore, each sample was significantly different from both *mohavensis* and *scirpensis*, but not *sanctidiegi*, by Tukey–Kramer post hoc tests derived from 1-way ANOVA (Table S6.1, Supplementary Data SD6). Overall, of 283 individual specimen assignments summed for

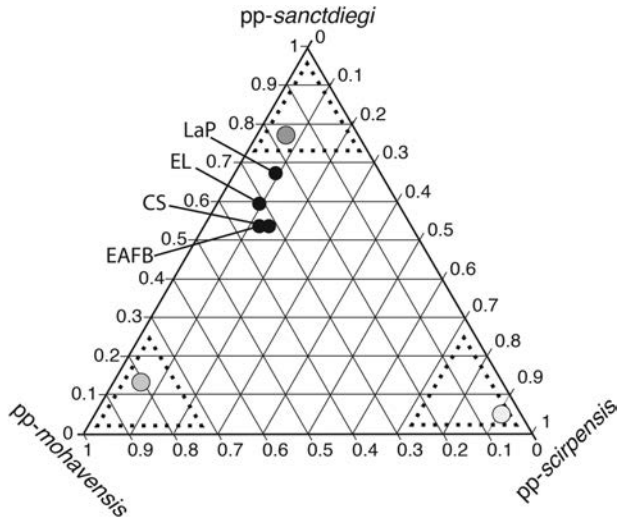

Fig. 6.—Mean sample posterior probabilities derived from canonical analyses of each of the 4 separate data sets for all southern samples of the California vole (*Microtus californicus*), with the 2 southern subspecies (*mohavensis* and *sanctidiegi*) plus *scirpensis* as a priori groups. The dotted triangles in each corner circumscribe the approximate 75% boundary for inclusion; the gray-filled circles represent the mean posterior probabilities for each of the 3 a priori subspecies (medium gray = *mohavensis*; dark gray = *sanctidiegi*; light gray = *scirpensis*); and the black circles are the mean posterior probabilities of group assignment for each of the 4 nonaligned localities, each identified by the locality acronym (CS = Cushenbury Springs; EAFB = Edwards Air Force Base; EL = Elizabeth Lake; and LaP = Lake Palmdale; see Fig. 2).

the 4 data sets, 76.7% (217) were classified as *sanctidiegi* and only 16.3% (46) as *mohavensis*; fewer than 7% were classified as *scirpensis* (Table S6.2, Supplementary Data SD6).

Concordance between morphology and molecules

We assessed the correspondence between an individual's morphological attributes and its molecular group membership by correlating posterior probabilities derived from each morphological data set and assignment probabilities based on microsatellite loci (from Conroy et al. 2016). As above, we performed separate analyses on the northern and southern sets of samples, including the a priori defined subspecies and all of the unassigned samples. We made these comparisons only for posterior probabilities with respect to *kernensis* and *vallicola* for the northern group and *mohavensis* and *sanctidiegi* for the southern group, excluding those to *scirpensis* in both cases as the latter had too few comparisons in common across the different data sets.

For the northern sample set, adjusted R^2 values between all pairwise comparisons of an individual's posterior probability of assignment to either *kernensis* or *vallicola* were high, with each adjusted R^2 significant and most highly so ($P < 0.0001$; Table S7, Supplementary Data SD7). Importantly, and with a single exception, the correspondence between an individual's genotype and its phenotype was highly significant (*kernensis* comparisons: R^2 values ranged from 0.1155, $P = 0.0001$ [microsat posterior probability to color posterior probability] to 0.5326, $P < 0.0001$ [microsat to craniodental]; *vallicola* comparisons: $R^2 = 0.1471$, $P < 0.0001$ [microsats to color] and 0.4114, $P < 0.0001$ [microsats to foramina]). The molecular genetic background of each individual, at least as identified by nuclear microsatellite loci, was reasonably predictive of the expression of morphological attributes of each individual, although differentially (mean R^2 for comparisons with *kernensis* was 0.5494; that with *vallicola* was 0.2915).

The southern group of samples contrasted sharply to those of the north with respect to the general concordance of individual assignments across the microsatellite and morphological data sets. Overall, only weak relationships were found between an individual's microsatellite and either craniodental or foramina posterior probabilities, but not for either color or qualitative craniodental traits (Table S7, Supplementary Data SD7). Adjusted R^2 values for both *mohavensis* and *sanctidiegi* assignments ranged from 0.0004 ($P = 0.84$; *mohavensis* microsat versus qualitative posterior probabilities) to 0.0818 ($P = 0.006$; *mohavensis* microsat versus craniodental probabilities).

The contrasting pattern of character relationships in northern versus southern samples, and the general decoupling between molecular and morphological characters sets in the southern ones, is not unexpected. Northern samples were rather cleanly divisible in both character sets into units that corresponded to the a priori defined subspecies *kernensis* and *vallicola*. On the other hand, across the southern samples, the division based on molecular assessment separated western samples on the flank of the San Gabriel Mts. and adjacent desert floor from those to the east, in the San Bernardino Mts. plus nearby desert samples (Fig. 1), but that based on morphological characters separated the geographically restricted subspecies *mohavensis* from all other samples (Fig. 4).

Discussion

The conundrum of subspecies: their definition and reality

The classification of organisms in use at any one point in time is a function of the taxonomic philosophy, kinds of data, and analytical means then in place. Today, taxonomy, the science of classification, is dominated by the application of phylogenetic principles first posited by Willi Hennig in 1966 (in the English translation of his book) and the almost universal use of molecular data. Two general principles underlying systematics today is that our taxonomy should reflect evolutionary history, and further, with respect to infraspecific taxa, that subspecies are qualitatively equivalent to species in their conceptual underpinning (see, for example, Zink 2004; Sackett et al. 2014; Trujillo and Hoffman 2017). Both principles stem directly from the application of modern molecular genetic techniques, but the first (history) is inappropriately limited to molecules and the second (species equivalency) is simply incorrect.

One result of this new paradigm and data shift has been the inevitable conflict when an existing taxonomy, based on the rules and approaches of an earlier era, meets the results of modern laboratory and analytical methodologies. Resolution of these conflicts at categorical levels above the species is relatively transparent through Hennig's cladistic methodology, but a rigid application of these same rules at infraspecific levels is often not possible nor is such even consistent with Hennigian principles. An increasing number of scholars today do not appear to appreciate this distinction.

As implemented in the early 20th century, subspecies were defined and diagnosed by geographic discontinuities in morphological traits within the range of a species under a polytypic species concept; some, although not all, believed such discontinuities to reflect evolutionary history (for example, see Grinnell 1935:403–404). By the mid part of the last century, the value of subspecies became contested for a variety of conceptual and empirical reasons (see contravening opinions by Wilson and Brown [1953] and Lidicker [1962], for example). Today, much of the infraspecific literature, as noted above, has become centered on delineating molecular clades that are geographically structured (phylogeography). Under this paradigm, however, most authors have either, or both, 1) lost sight of the fact that morphological attributes also have a genetic basis, and thus have a history unto their own, or 2) the requirement of clade structure upon which an intraspecific taxonomy is to be based is actually contrary to Hennig's own beliefs. Hennig (1966:18) recognized that "the structure of the genealogical relationships within the species does not correspond to the definition of a hierarchical system...", and thus subspecies, for example, cannot be equated exactly to the ordered hierarchy of higher taxa, like the species. Why? Because relationships within species remain governed by reproductive compatibilities that promote gene flow, which itself can only be disrupted by population

(variance in effective population size, philopatry, assortative mating, sex-biased dispersal) or ecological processes (habitat-based density troughs, absolute vicariant barriers). Subspecies are genealogical networks of populations, often without cladistic structure; species, on the other hand, are hierarchical units with a dichotomous branching history.

Hennig (1966:55–56) succinctly expressed his view of subspecies in the following: "The ultimate aim of taxonomy at the species level must be to recognize and distinguish as subspecies all vicarying reproductive communities, at least insofar as ... these are not merely externally limited but also have definite distinguishing characters. Such distinguishing characters need not be purely morphological. It is entirely possible for vicarying subspecies to *differ only statistically* (emphasis ours), with certain variants ... appearing in different frequencies in two spatially separated reproductive communities." This conceptual framework defines a nonhierarchical, nonreciprocal monophyletic definition for infraspecific taxa. Braby et al. (2012:699), in a cogently argued review of infraspecific taxa in a group of butterflies, expanded on Hennig's views and defined subspecies as "groups that comprise evolving populations representing partially isolated lineages of a species that are allopatric, phenotypically distinct ... and that these character differences are (or are assumed to be) correlated with evolutionary independence according to population genetic structure."

These views of subspecies as coordinate units distributed in space and with independent histories allow them to be defined by either, or both, morphological and molecular attributes. Furthermore, these views recognize that infraspecific taxa defined by explicitly stated diagnosable criteria in the past, and whose names are thus governed by the rules of nomenclature, have relevance today as testable hypotheses by the application of, but not replacement by, additional character analyses. These views should also force us to remember that all phenotypic attributes, be these morphological or molecular, are governed by their underlying genetic background. Furthermore, if population segments (i.e., subspecies) have separate evolutionary histories, so may the characters that diagnose these segments. Characters, as do populations, respond differentially to the complexity of stabilizing, disruptive, divergent, or even neutral evolutionary processes. These separate character histories are thus also likely to be in conflict, the result of which will be discordance in geographic patterning. The formal recognition of subspecies should focus on both the documentation and assessment of this almost inevitable discordance, not on the rigid adherence to a molecular-only view of history (e.g., Zink 2004; Brenneman et al. 2016; Trujillo and Hoffman 2017).

The necessity to resolve conflict might be unsettling to some, but nature rarely conforms to simplistic expectations; indeed, we can expect nature to be "messy." Hence, the philosophy espoused by an investigator must deal with the realities of working to reconcile an existing taxonomy in the face of conflict, for example, and by appropriately evaluating the diagnoses upon which that taxonomy was based rather than simple dismissal of that taxonomy as in error because it now conflicts with newly assessed data.

Why is the realization of both definition and applicability of the subspecies concept important? First, the entire scientific enterprise of taxonomy is based on fundamental attributes of human nature—our desire to recognize, describe, conceptually organize, and name the discontinuities we observe in nature (Berlin et al. 1973; see also the cogent arguments given by Remsen [2010] regarding avian subspecies). And second, because infraspecific taxa defined long ago are often the basis for legal decisions regarding threatened or endangered status, and thus they underpin management plans developed to mitigate severe declines. Scholars thus have the obligation to evaluate all data available as effectively as possible and to reach conclusions regarding intraspecific taxa, their definition and diagnosis, based on the principles that Hennig himself elaborated.

Taxonomy of desert Microtus californicus

Conroy et al. (2016) delineated 5 spatially separated reproductive communities of California voles within the Mojave Desert and adjacent mountain ranges, each defined by a shared genetic heritage and a singular geographic range (see Fig. 1). And, as we document above, these communities also differ statistically in 4 separate morphological character data sets. The degree to which they differ, however, is not uniform, nor is the strength of difference separating them uniform across the data sets (Fig. 4). Nonetheless, each geographic entity conforms to the definitions of infraspecific taxa given by Hennig (1966), and as elaborated by Braby et al. (2012).

These taxa were formally named nearly a century or more ago. Despite the few specimens and limited character sets, as well as the lack of sophisticated analytical methods then available, those early workers were remarkably perceptive in their recognition of distinct entities that now prove to have unitary geographic ranges and expanded sets of diagnosable morphological characters. And, as Conroy et al. (2016) documented, all 5 groups can be defined by molecular analyses using a combination of mitochondrial DNA sequences and nuclear microsatellite loci, even if both molecular sets are themselves partly in conflict. Furthermore, in the course of our study we have substantially expanded the ranges of 2 of these taxa onto the desert floor and, in so doing, have refined their geographic as well as morphological and molecular boundaries. Our analyses of these desert floor samples also allow for relatively well-supported assignments of each to a priori defined subspecies bordering or within the deserts of eastern California, but also point to samples from geographically intermediate regions that are, themselves, somewhat intermediate in morphology and thus difficult to assign. Such is the expected nature of intraspecific patterns, and we leave it to future studies, with expanded samples of specimens and data sets for further resolution.

Here, we provide an emended diagnosis of each subspecies of California vole in the Mojave Desert or in adjacent highland areas based on our character analyses, comparisons to other subspecies, and geographic range. We exclude *M. c. sanctidiegi* from the following as our analyses included only samples from the Transverse Ranges, which is both a small part of an otherwise large geographic range in southern California and does

not include the type locality (Kellogg 1918; Hall 1981). Tables 1–4 provide character summaries (mean or median, standard error, range, and sample size) for each subspecies for external and craniodental variables, colorimetric measurement, foramina, and qualitative craniodental scores, respectively.

Microtus californicus kernensis Kellogg
Kern River Vole

Microtus californicus kernensis Kellogg, 1818:26; type locality "Fay Creek, 4100 feet altitude, Kern County, California." Fay Creek is a small stream draining into the north bank of South Fork of the Kern River at Weldon, east of Lake Isabella in South Fork Valley; approximate coordinates 35.7412N, 118.3100W.

Emended diagnosis.—A member of the Northern mtDNA clade and Kern River nuclear microsatellite group (Fig. 1; Conroy et al. 2016). Second largest among the taxa compared in external dimensions (mean TOL = 193.7 mm, mean HB = 133.4 mm) with a relatively long tail (ratio of tail to head-and-body length = 45.2%), otherwise generally intermediate values in most craniodental measurements except for having the narrowest interparietal (mean IPW = 7.38 mm; Table 1). Mean adult dorsal color closest to the Munsell color descriptor "very dusky red" (2.5YR/2.5/2), with overall range between "very dark brown" (10YR/2/2) and "very dusky red" (2.5YR/3/2). The subadult pelage shares the same color parameters as the adult pelage. Overall, *kernensis* shares the same colorimetric values as *mohavensis* (Table 2). The majority of specimens possess a maxillary foramen (70 of 74 = 94.6%); equal numbers either lack or possess squamosal foramina (85.1%); most (39 of 74 = 52.7%) have a single hypoglossal foramen, or single on one side but double on the other (24 of 74 = 32.4%); and evenly represented single enlarged, multiple small, or both posterior palatal fenestrae (Table 3). The majority of specimens have proodont upper incisors (60 of 89 = 67.4%), an elongated premaxilla extension (61 of 89 = 68.5%), strong taper (64 of 89 = 71.9%) and notched posterior end of the nasals (55 of 89 = 61.8%), oval incisive foramina (73 of 89 = 82.0%) but shortened premaxillary septum (78 of 89 = 87.6%), double posterior loop on M2 (85 of 89 = 95.5%), weakly to strongly present labial 4th tine on M3 (84 of 80 = 94.4%), and weak to no lingual indentation on M3 (82 of 89 = 91.1%; Table 4).

Comparisons.—*Microtus c. kernensis* differs from *M. c. vallicola* by having a significantly longer skull with longer nasals, longer incisive foramina, longer 3rd maxillary molars, and by being wider across both the zygomatic arches and mastoid regions; dorsal pelage with same overall very dusky red color but range to dark brown rather than blackish tones; maxillary foramen present in the majority of specimens, and more specimens with an enlarged posterior palatal opening on 1 or both sides; a larger proportion of specimens with an elongated premaxillary portion of the incisive foramina septum; and a greater proportion of specimens with weakly indented labial surface of M3. Otherwise, these 2 subspecies share similar foraminal and qualitative craniodental character frequencies.

Microtus c. kernensis is uniformly smaller in most cranial dimensions relative to *M. c. scirpensis*, particularly in cranial length, nasal width, interparietal width, palatal length, molar toothrow length, mandibular length, and lengths of both 1st and 2nd upper molars; dorsal pelage with more brownish to reddish rather than dark brown to blackish tones; a higher proportion of specimens have the maxillary foramen present on both sides, a single hypoglossal foramen, and more even distribution of single or multiple posterior palatal fenestrae; and a larger proportion of specimens have an oval as opposed to distally tapered or expanded incisive foramina, weakly to strongly developed M3 labial 4th tine, and weakly or deeply indented M3 lingual indentation.

In craniodental dimensions, *M. c. kernensis* differs only minimally from *M. c. mohavensis*, with significantly narrower nasals and interparietal, shallower crania, but longer 3rd upper molars; the 2 also share similar dusky red dorsal color tones; significantly higher frequency of specimens have squamosal and maxillary foramina, a single hypoglossal foramen predominantly present on 1 or both sides, and uniform distribution of single or multiple posterior palatal fenestrae; and most have proodont as opposed to orthodont upper incisors, strongly tapered and notched rather than parallel and squared posterior ends to the nasals, oval rather than distally tapered incisive foramina, double rather than single posterior loop on M2, weakly to strongly developed 4th tine on M3 rather than no or only weakly expressed ones, and weakly indented lingual surface on M3 rather than a smooth surface.

In comparison to Transverse Range *M. c. sanctidiegi*, *M. c. kernensis* has significantly longer skulls, longer but narrower interparietals, longer incisive foramina, palates, mandible, and all 3 upper molars, but has wider nasals, zygomatic breadth, and interorbital region; overall dorsal pelage tones dusky red rather than reddish brown; a significantly higher proportion of individuals have no squamosal foramen, a maxillary foramen present on both sides, a single hypoglossal foramen, and a single enlarged posterior palatal fenestra; and a significantly higher number of individuals with proodont upper incisors, a long premaxillary extension, strongly tapered and notched posterior ends of the nasals, oval incisive foramina with short premaxillary portion to the septum, a double loop on M3, weakly to strongly developed 4th tine on M3, and weakly to deeply indented lingual surface on M3.

Range.—The Kern River Plateau at the southern terminus of the Sierra Nevada, including the drainages of the Kern River, South Fork Kern River, Canebrake Creek, and Spanish Needle Creek, south to encompass the high elevations of the Piute Mts., Walker Basin, Tehachapi Valley, and Tehachapi Mts. The region further to the west around the southern end of the San Joaquin Valley and vicinity of Mt. Pinos, included by Kellogg (1918) and Grinnell (1933) in the overall range of *M. c. kernensis* is part of a broad intergrade zone between mixtures of both Southern and Northern mtDNA haplotypes (Conroy and Gupta 2011). The western margin of the range is perhaps best placed in the Fort Tejon-Lebec areas in Grapevine Canyon.

Table 1.—Descriptive statistics for external and craniodental variables of pooled samples of 5 taxa of California desert *Microtus californicus* (mean, standard error, sample size, and range). Variables are defined in "Materials and Methods."

Variable	*kernensis*[a]	*mohavensis*	*sanctidiegi*	*scirpensis*[b]	*vallicola*[b]
TOL	193.70 ± 1.324	189.30 ± 2.068	181.53 ± 1.628	202.38 ± 4.329	181.97 ± 1.482
	n = 105	*n* = 23	*n* = 76	*n* = 8	*n* = 77
	155–227	166–208	153–215	187–222	153–221
TAL	60.28 ± 0.555	59.00 ± 0.958	54.50 ± 0.663	60.75 ± 2.852	55.55 ± 0.667
	n = 105	*n* = 23	*n* = 76	*n* = 8	*n* = 77
	47–75	50–70	42–68	48–76	40–68
HB	133.43 ± 1.039	130.03 ± 1.423	127.03 ± 1.201	141.63 ± 3.235	126.43 ± 1.124
	n = 105	*n* = 23	*n* = 76	*n* = 8	*n* = 77
	102–162	116–141	101–154	127–157	105–146
HF	23.45 ± 0.246	23.48 ± 0.198	22.30 ± 0.193	24.00 ± 0.423	23.66 ± 0.161
	n = 106	*n* = 23	*n* = 76	*n* = 8	*n* = 77
	19–27	22–25	19–26	22–26	21–29
E	16.81 ± 0.118	16.80 ± 0.374	16.21 ± 0.119	13.88 ± 0.875	14.07 ± 0.296
	n = 103	*n* = 23	*n* = 76	*n* = 8	*n* = 76
	14–20	16–18	14–18	11–18	9–18
CIL	30.29 ± 0.121	30.38 ± 0.247	29.39 ± 0.163	32.83 ± 0.348	29.44 ± 0.149
	n = 106	*n* = 23	*n* = 76	*n* = 8	*n* = 80
	26.98–33.16	27.73–32.51	26.10–32.09	31.30–34.21	26.81–32.10
NL	9.15 ± 0.052	9.34 ± 0.100	9.01 ± 0.066	9.75 ± 0.183	8.63 ± 0.063
	n = 106	*n* = 23	*n* = 79	*n* = 8	*n* = 80
	7.64–10.634	8.34–10.12	7.74–10.15	8.79–10.52	7.29–9.93
NW	3.65 ± 0.023	3.91 ± 0.038	3.50 ± 0.025	4.31 ± 0.078	3.77 ± 0.034
	n = 106	*n* = 23	*n* = 79	*n* = 8	*n* = 80
	2.90–4.21	3.51–4.24	2.97–3.96	4.08–4.74	3.16–4.51
ZB	17.38 ± 0.074	17.08 ± 0.151	16.80 ± 0.112	18.63 ± 0.227	16.82 ± 0.109
	n = 106	*n* = 23	*n* = 79	*n* = 8	*n* = 80
	15.59–19.20	15.85–18.31	14.37–18.91	17.63–19.83	14.49–18.85
IOC	3.71 ± 0.020	3.60 ± 0.025	3.53 ± 0.025	3.60 ± 0.035	3.74 ± 0.018
	n = 106	*n* = 23	*n* = 79	*n* = 8	*n* = 80
	3.23–4.32	3.38–3.97	3.01–4.15	3.44–3.77	3.45–4.22
IPW	7.38 ± 0.043	8.27 ± 0.128	7.80 ± 0.047	8.33 ± 0.172	8.01 ± 0.058
	n = 106	*n* = 23	*n* = 79	*n* = 8	*n* = 80
	6.41–8.94	6.77–9.24	6.33–8.56	7.29–8.92	6.92–9.22
IPL	3.69 ± 0.044	3.55 ± 0.069	3.49 ± 0.042	4.29 ± 0.164	4.16 ± 0.042
	n = 106	*n* = 23	*n* = 79	*n* = 8	*n* = 80
	2.23–4.94	2.66–4.36	2.64–4.31	3.54–5.00	3.45–5.14
BPL	15.18 ± 0.070	15.16 ± 0.154	14.66 ± 0.088	16.91 ± 0.177	14.94 ± 0.087
	n = 106	*n* = 23	*n* = 79	*n* = 8	*n* = 80
	13.84–17.48	13.42–16.78	13.01–16.32	16.32–17.97	13.36–17.43
IFL	5.74 ± 0.031	5.66 ± 0.073	5.52 ± 0.048	5.88 ± 0.058	5.33 ± 0.039
	n = 106	*n* = 23	*n* = 79	*n* = 8	*n* = 80
	4.92–6.45	5.49–6.35	4.54–6.37	5.66–6.13	4.69–6.49
MB	13.28 ± 0.051	13.38 ± 0.094	13.14 ± 0.063	13.94 ± 0.224	12.87 ± 0.068
	n = 106	*n* = 23	*n* = 79	*n* = 8	*n* = 80
	11.88–14.59	12.32–14.66	11.45–14.21	13.13–15.27	11.63–14.49
MTRL	7.41 ± 0.033	7.51 ± 0.070	7.33 ± 0.042	8.08 ± 0.091	7.55 ± 0.051
	n = 106	*n* = 23	*n* = 79	*n* = 8	*n* = 80
	6.53–8.26	6.87–8.12	6.61–8.21	7.77–8.53	6.51–8.57
CD	10.91 ± 0.033	11.19 ± 0.061	10.90 ± 0.054	11.36 ± 0.136	10.97 ± 0.054
	n = 106	*n* = 23	*n* = 79	*n* = 8	*n* = 80
	10.18–11.75	10.79–12.07	9.66–12.10	10.77–11.96	9.88–12.37
ManL	18.12 ± 0.076	18.11 ± 0.163	17.36 ± 0.110	19.76 ± 0.302	17.98 ± 0.112
	n = 106	*n* = 23	*n* = 79	*n* = 8	*n* = 80
	16.54–20.03	16.60–19.56	15.44–19.59	18.52–21.28	16.11–20.02
L-M1	2.755 ± 0.0144	2.738 ± 0.0306	2.609 ± 0.022	3.194 ± 0.038	2.740 ± 0.0223
	n = 106	*n* = 23	*n* = 79	*n* = 8	*n* = 80
	2.333–3.183	2.542–3.022	2.148–3.162	3.063–3.411	2.176–3.233
L-M2	1.981 ± 0.0097	1.984 ± 0.0221	1.913 ± 0.0148	2.216 ± 0.0385	2.011 ± 0.0168
	n = 106	*n* = 23	*n* = 79	*n* = 8	*n* = 80
	1.703–2.308	1.823–2.157	1.678–2.250	2.060–2.3671	1.626–2.423
L-M3	2.361 ± 0.0157	2.232 ± 0.0297	2.133 ± 0.024	2.499 ± 0.0602	2.274 ± 0.0190
	n = 106	*n* = 23	*n* = 79	*n* = 8	*n* = 80
	1.992–2.841	1.937–2.459	1.201–2.502	2.253–2.767	1.846–2.608

[a]Excludes intermediate sample from Owens Lake (OL).
[b]Excludes intermediate sample from Saline Valley (SV).

Table 2.—CIE colorimetric variables (mean ± *SE*, range, and sample size) with corresponding mean and range of Munsell values for the 5 taxa of California desert *Microtus californicus* (*n* = sample size). Variables are defined in "Materials and Methods."

Variable	*kernensis* (*n* = 67)	*mohavensis* (*n* = 40)	*sanctidiegi* (*n* = 21)	*scirpensis* (*n* = 9)	*vallicola* (*n* = 117)
CIE-X	5.466 ± 0.124	5.079 ± 0.156	6.761 ± 0.210	3.827 ± 0.456	4.265 ± 0.083
	3.31–8.65	3.48–8.03	4.43–8.40	1.79–6.07	1.79–6.07
CIE-Y	5.551 ± 0.131	5.148 ± 0.162	6.916 ± 0.221	3.878 ± 0.458	4.328 ± 0.085
	3.33–8.88	3.45–8.27	4.51–8.62	1.84–6.13	1.96–6.41
CIE-Z	3.704 ± 0.121	3.420 ± 0.146	5.026 ± 0.191	3.102 ± 0.319	3.104 ± 0.076
	1.95–6.31	1.82–6.82	3.26–6.54	1.71–4.60	1.46–5.11
Munsell mean	2.5YR/2.5/2	2.5YR/2.5/2	5YR/3/2	10YR/2/1	2.5YR/2.5/2
	very dusky red	very dusky red	dark reddish brown	black	very dusky red
Munsell range	10YR/2/2	10YR/2/2	2.5YR/2.5/2	10YR/2/1	10YR/2/1
	very dark brown	very dark brown	very dusky red	black	black
	to	to	to	to	to
	2.5YR/3/2	2.5YR/3/2	2.5YR/3/2	7.5YR/3/2	2.5YR/3/2
	dusky red	dusky red	dusky red	dark brown	dusky red

Table 3.—Frequency of foramina in 5 taxa of California desert *Microtus californicus*, including core samples only of each subspecies.

Foramen/condition	*kernensis* (*n* = 74)	*mohavensis* (*n* = 45)	*sanctidiegi* (*n* = 23)	*scirpensis* (*n* = 23)	*vallicola* (*n* = 106)
Squamosal foramen (SqF)					
Median/mean	2/2.041	1/1.422	3/2.435	3/2.261	2/1.830
Absent	30	32	5	6	52
Present—1 side only	11	7	3	5	20
present—both sides	33	6	15	12	34
Maxillary foramen (MaxF)					
Median/mean	3/2.932	2/1.912	2/1.870	1/1.261	1/1.236
Absent	1	17	10	19	90
Present—1 side only	3	15	6	2	7
Present—both sides	70	13	7	2	9
Hypoglossal foramen (HypoF)					
Median/mean	1/1.621	3/2.578	3/2.478	2/2.087	2/1.821
Single	39	6	3	8	49
Single/double	24	7	6	5	27
Double	11	32	14	10	30
Posterior palatal fenestrae (MPF)					
Median/mean	2/2.027	3/2.622	3/2.435	2/1.957	3/2.472
Single	23	5	4	3	8
Single—1 side	26	7	5	18	40
Multiple	25	33	14	2	58

This subspecies extends onto the floor of the Mojave Desert in scattered pockets of mesic vegetation along canyons on the eastern slope of the Scodi Mts. (Freeman Canyon) and southern margins of the Sierra Nevada (Sand Canyon, Ninemile Canyon, and probably others not presently surveyed), and north to Little Lake. We allocate specimens from the extreme southern end of Owens Lake (Olancha Creek and Cartago) to *M. c. kernensis* based on their overwhelming morphological character sharing (Fig. 5), even though the molecular assignments of these specimens reflect strong admixture with *M. c. vallicola* from the Owens Valley (see results above and Conroy et al. 2016). This subspecies extends eastward into isolated wetland pockets on China Lake Naval Air Weapons Station in Indian Wells Valley and Upper and Lower Haiwee Spring on the western slope canyons of the Coso Range; it is likely present in similar small wetland patches elsewhere in the Coso Range and possibly eastward into the adjacent Argus Range.

Microtus californicus vallicola Bailey
Owens Valley Vole

Microtus californicus vallicola Bailey, 1898:89; type locality "Lone Pine, Inyo Co., California"; coordinates approximately 36.60636N, 118.06900W.

Emended diagnosis.—A member of the Northern mtDNA clade and Owens Valley nuclear microsatellite group (Fig. 1; Conroy et al. 2016), *M. c. vallicola* is one of the smallest in body size (mean TOL = 181.97 mm; mean HB = 126.43), and has an absolutely short tail (mean TAL = 55.6 mm), and with small values of most craniodental measurements, notably short nasal bones (mean NL = 8.63 mm), short incisive foramina (mean IFL = 5.33 mm), and narrow braincase (mean MB = 12.87 mm; Table 1). Mean adult dorsal color is closest to Munsell color "very dusky red" (2.5YR/2.5/2), with the overall range between "black" (10YR/2/1) and "dusky red" (2.5YR/3/2; Table 2). Subadult pelage of young animals

Table 4.—Frequency of qualitative craniodental traits in 5 taxa of California desert *Microtus californicus*.

Character/state	*kernensis* (*n* = 89)	*mohavensis* (*n* = 47)	*sanctidiegi* (*n* = 27)	*scirpensis* (*n* = 14)	*vallicola* (*n* = 128)
Procumbency					
Median/mean	2/1.674	1/1.043	1/1.222	2/1.786	2/1.758
Orthodont [1]	29	45	21	3	31
Proodont [2]	60	2	6	11	97
Premax extension					
Median/mean	2/1.1685	2/1.702	2/1.852	2/1.643	2/1.679
Short [1]	28	14	5	5	43
Long [2]	61	33	22	9	85
Nasal posterior taper					
Median/mean	2/1.719	1/1.085	1/1.111	2/1.714	2/1.711
Parallel or weak [1]	25	43	24	4	37
Strong [2]	64	4	3	10	91
Posterior nasal end					
Median/mean	3/2.236	1/1.213	1/1.296	3/2.214	3/2.281
Squared [1]	34	42	23	5	44
Notched [2]	55	5	4	9	84
Incisive foramina shape					
Median/mean	1/1.281	3/2.404	3/2.519	2/2.000	1/1.148
Oval [1]	73	13	5	5	112
Distally tapered [2]	7	2	3	4	13
Distally expanded [3]	9	32	19	5	3
Premax portion of septum					
Median/mean	1/1.124	1/1.340	2/1.704	2/2.000	2/1.625
Short	78	31	8	2	51
Long	11	16	19	12	77
Postero loph of M2					
Median/mean	2/1.955	1/1.021	1/1.000	2/1.857	2/1.969
Single loop [1]	4	46	27	2	4
Double loop [2]	85	1	0	12	124
M3 labial 4th tine					
Median/mean	2/2.281	1/1.128	1/1.296	1/1.214	2/1.672
Not present [1]	5	41	20	11	52
Weakly present [2]	54	6	6	3	66
Strongly present	30	0	1	0	10
M3 lingual indentation	2/1.831	1/1.234	1/1.370	1/1.214	1/1.438
No indentation [1]	22	36	17	11	74
Weakly indented [2]	60	11	10	3	52
Deeply indented [3]	7	0	0	0	2

expresses the same color parameters as the adult pelage. Most specimens lack both the squamosal (52 of 106 = 49.1%) and maxillary foramina (90 of 106 = 84.9%) but possess a single hypoglossal foramen (50 of 106 = 47.2%) and multiple posterior palatal pits (59 of 106 = 55.7%; Table 3). The majority have proodont upper incisors (97 of 128 = 75.8%), a long premaxillary extension (85 of 128 = 66.4%), strongly tapered posterior nasal margins (91 of 128 = 71.1%) that have a medial notch (84 of 128 = 65.6%), oval incisive foramina (112 of 128 = 87.5%) with a long premaxillary part of the septum (77 of 128 = 60.2%), and upper cheekteeth with a double posterior loop on M2 (124 of 128 = 96.9%), either no or a only a weakly present labial 4th tine on M3 (118 of 128 = 92.2%), and either lack or have only a weakly indented lingual surface of M3 (126 of 128 = 98.4%; Table 4).

Comparisons.—Characters separating *M. c. vallicola* from adjacent *M. c. kernensis* are given above. Relative to *M. c. scirpensis*, *M. c. vallicola* is significantly smaller in most (11 of 16) craniodental dimensions, with notably shorter incisive foramina and 3rd upper molars; average adult dorsal pelage color is dusky red rather than more blackish; shares similar patterns in the expression of squamosal, maxillary, and hypoglossal foramina but differs in having a significantly higher proportion of multiple equal-sized posterior palatal fenestrae; and shares similar proodont upper incisors, premaxillary extensions, tapered and notched posterior nasal ends, double posterior loph on M2, lack of or only weakly developed 4th tine on M3, and smooth lingual surface of M3, but differs significantly in its oval incisive foramina and long premaxillary septum.

Microtus c. vallicola differs from *M. c. mohavensis* by having a significantly shorter skull, with shorter nasals and incisive foramina, and a narrower mastoid breadth, but wider across the interorbital region and has a longer interparietal; typical dorsal pelage color is dusky red, with more blackish than dark brown tones; it shares similar patterns of the squamosal foramen and multiple rather than single enlarged posterior palatal fenestrae but differs in usually lacking the maxillary foramen and having a single rather than double hypoglossal foramen, proodont rather than orthodont upper incisors, tapered and notched

posterior nasal ends, oval as opposed to distally expanded incisive foramina with a long rather than short premaxillary septum, a double (not single) posterior loph on M2, lack of or only weakly developed 4th tine on the labial surface of M3, and smooth or only weakly indented lingual surface of M3.

In comparison to Transverse Range *M. c. sanctidiegi*, *M. c. vallicola* has significantly shorter nasals and incisive foramina, narrower mastoid breadth, but wider nasals and interorbital region, and longer interparietal, maxillary tooth rows, mandible, and all 3 maxillary molars; overall dorsal pelage with dusky red rather than reddish brown tones; largely absent as opposed to usually present squamosal foramen, usually absent rather than equally present maxillary foramen, usually single rather than double hypoglossal foramen, but share similar multiple equal-sized posterior palatal fenestrae; and proodont versus orthodont upper incisors, tapered and notched rather than parallel and squared posterior nasal ends, oval opposed to distally expanded incisive foramina, double (not single) posterior loph on M2, but share similar weak to no development of the 4th labial tine and rather smooth lingual surface on M3.

Range.—Known from multiple localities on the floor of the Owens Valley, including the lower drainages flowing from both the Sierra Nevada on the west and White-Inyo mountains on the east, from the northern fringe of Owens Lake to at least Round Valley, Fish Slough, and the mouth of Silver Canyon north and northeast of Bishop. Populations from the southern wetlands of Owens Lake at Cartago are allocated to *M. c. kernensis* (see above). *Microtus c. vallicola* extends into the isolated Deep Springs Valley between the White and Inyo mountains, with known localities at Antelope Spring in the northwestern and Wyman Creek in the northeastern corners. The Owens Valley vole is syntopic with the montane vole (*Microtus montanus*) in Round Valley northwest of Bishop and Fish Slough north of Bishop, and co-occurs with both the montane vole and long-tailed vole (*Microtus longicaudus*) along Wyman Creek in Deep Springs Valley. Interestingly, this taxon is apparently not present in vicinity of the numerous springs that surround Deep Springs Lake, and from which only the montane vole has been caught. Pending the availability of additional specimens and new analyses, the range of *M. c. vallicola* might extend to localities in and around Saline Valley east of the Inyo Mts.; current data indicate these samples are intermediate between *M. c. vallicola* and *M. c. scirpensis* (e.g., Fig. 5). Currently listed as a Species of Special Concern by the California Department of Fish and Wildlife.

Microtus californicus scirpensis Bailey
Amargosa Vole

Microtus scirpensis Bailey, 1900:38: type locality "Amargosa River (near Nevada Line), Inyo County, Calif."; subsequently understood to be "a small tule [*Scirpus olneyi*] marsh at a spring near Shoshone on the Amargosa River, in eastern Inyo County. Altitude of station 1500 to 1600 feet; zonal range Lower Sonoran" (Kellogg 1918:24); coordinates approximately 35.97690N, 116.27516W.

Microtus californicus scirpensis: Kellogg, 1818:24; current name combination.

Emended diagnosis.—A member of the Southern mtDNA clade but with a nuclear microsatellite array equally divergent to those of other taxa (Fig. 1; Conroy et al. 2016); may have originated by dual pathways from both an older Owens Valley connection (late Pleistocene) via Owens Lake, Searles Lake, Panamint Lake, and Amargosa River basin in Death Valley and a younger connection (Holocene) with the Mojave River drainage to the south (see Conroy et al. 2016). This is the largest of the 5 taxa in the Mojave Desert in body size (mean TOL = 202.4 mm; mean HB = 141.6 mm), with the longest tail (mean TAL = 60.8 mm), and largest in nearly all craniodental dimensions (means of all variables are significantly largest, except IOC; Table 1). Dorsal color is the darkest of desert California voles, with a mean adult dorsal color closest to Munsell color "black" (10YR/3/1); overall range between "black" (10YR/2/1) and "dark brown" (7.5YR/3/2). *M. c. scirpensis* is unique in that the subadult pelage of young animals is uniformly black, lacking any of the dark reddish infusion that characterizes adults (Table 2). Most specimens (19 of 23 = 82.6%) lack a maxillary foramen but possess the squamosal foramen (12 of 23 = 52.2%), have either a double or laterally asymmetrical single or double hypoglossal foramen (15 of 23 = 65.2%), and have asymmetrical posterior palatal fenestrae (18 of 23 = 78.2%) with a single large posterior palatal opening on one side but multiple fenestrae of equal size on the other (Table 3). Most specimens have proodont upper incisors (11 of 14 = 78.6%), a long premaxillary extension (9 of 14 = 64.3%), distally strongly tapered (10 of 14 = 71.4%) and notched (9 of 14 = 64.3%) nasals; even frequencies of incisive foramina shape but with a long (12 of 14 = 85.7%) premaxillary septum; a doubled posterior loph on M2 (12 of 14 = 85.7%), and lack of the labial 4th tine (11 of 14 = 78.6%) but smooth lingual surface (11 of 14 = 78.6%) of M3 (Table 4).

Comparisons.—Comparisons with *M. c. kernensis* and *M. c. vallicola* are given in those accounts. *Microtus c. scirpensis* shares more characters with *M. c. mohavensis*, but still has significantly longer skulls, nasals, palate, mandible, and upper molars with wider zygomatic arches and interparietal; it differs in its generally dark blackish dorsal adult pelage as opposed to dusky red tones, present rather than usually absent squamosal foramen; a higher proportion lack a maxillary foramen, have a double hypoglossal foramen, and a single enlarged as opposed to multiple equal-sized posterior palatal fenestrae; proodont rather than orthodont upper incisors; long rather than short premaxillary extensions; tapered and notched rather than parallel and squared posterior nasal ends; equal proportions of oval, distally tapered, or distally expanded incisive foramina rather than more typically distally expanded ones; a long rather than short premaxillary septum; and a double (not single) posterior loph on M2; but share a similar lack of or only weakly developed 4th labial tine and lingual indentation on M3.

From Transverse Range samples of *M. c. sanctidiegi*, *M. c. scirpensis* differs by being significantly larger in all dimensions except incisive foramina length and interorbital width; blackish rather than dark reddish brown dorsal pelage tones; shares usually present squamosal and maxillary

foramina, similar doubled hypoglossal foramen, but usually single enlarged as opposed to predominantly multiple equal-sized posterior palatal fenestrae; proodont rather than orthodont upper incisors; tapered and notched rather than parallel and squared distal nasal end; equal proportions of oval, distally tapered, or distally expanded incisive foramina rather than more typically distally expanded ones; double rather than single posterior loph on M3; but share similar development of the labial 4th tine and generally smooth lingual surface of M3.

Range.—Historically known from the type locality, a spring at the present town of Shoshone adjacent to the dry Amargosa River, to the hot springs at Tecopa about 13 km to the SSE, but now restricted to the latter. Federally listed as Endangered.

Microtus californicus mohavensis Kellogg
Mojave River Vole

Microtus californicus mohavensis Kellogg, 1918:29; type locality "Victorville, 2700 feet altitude, San Bernardino Co., California"; coordinates 34.53375N, 117.28750W.

Emended diagnosis.—A member of the Southern mtDNA clade and nuclear microsatellite group that also includes samples of *M. c. sanctidiegi* from the adjacent San Bernardino Mts. (Fig. 1; Conroy et al. 2016). Intermediate in overall body size between the large *M. c. scirpensis* and *M. c. kernensis* and the smaller *M. c. sanctidiegi* (samples from the adjacent Transvers Range) and *M. c. vallicola* (mean TOL = 189.3 mm; mean HB = 130.0 mm), but also with a long tail (mean TAL = 59.0 mm). Craniodental variables are unremarkable, but notable for being generally intermediate in most external and craniodental dimensions relative to the other 4 subspecies (Table 1). Mean adult dorsal color varies approximating "dusky red" (2.5YR/2.5/2) with individual specimens ranging from "dark brown" (10YR/2/2) to "dusky red" (2.5YR/3/2). Subadults have the same pelage color parameters as the adults. Overall, dorsal color is most similar to that of *M. c. kernensis* (Table 2). Most individuals lack a squamosal foramen (32 of 45 = 71.1%) but have a double hypoglossal foramen (32 of 45 = 71.1%), multiple posterior palatal openings (33 of 45 = 73.3%), and nearly equal representations of absent, present, or both maxillary foramina (Table 3). Most specimens (45 of 47 = 95.7%) have orthodont upper incisors, a long premaxillary extension (33 of 47 = 70.2%), parallel (43 of 47 = 91.5%) and squared (42 of 47 = 89.4%) posterior ends to the nasals, distally expanded (32 of 47 = 68.1%) incisive foramina with a short (31 of 47 = 66.0%) premaxillary septum, a single loop on the posterior loph on M2 (46 of 47 = 97.9%), and either lack or have only weakly developed labial 4th tine and indentation on lingual surface of M3 (Table 4).

Comparisons.—See above for comparisons with *M. c. kernensis*, *M. c. vallicola*, and *M. c. scirpensis*. From the nearby Transverse Range *M. c. sanctidiegi*, *M. c. mohavensis* differs by being significantly larger in body size, with a longer skull, nasals, palate, maxillary toothrows, mandible, and both the 1st and 2nd upper molars; a larger interparietal (both dimensions); and wider nasals, zygomatic breadth, and mastoid breadth, and deeper skull; dorsal color dusky red instead of dark reddish brown; squamosal foramen usually absent as opposed to present, but both taxa share similar frequencies for the 3 other foramina characters; and the 2 subspecies share nonsignificantly different counts for most qualitative craniodental characters except for having short as opposed to long premaxillary septum of the incisive foramen.

Range.—Known only from the margins of the Mojave River at 2 points about 8 km distant on the floor of the Mojave Desert just north of the San Bernardino Mts. in San Bernardino County: 1) an approximate 5-km stretch of the river in Victorville, where the river cuts through a granite hill and thus where bedrock close to the surface prevents water from disappearing into the sand; and 2) north of Oro Grande, along a stretch of approximately 6 km where the groundwater table is sufficiently shallow to allow water to flow continuously and to support a wide (up to 0.6 km) riparian community. The natural vegetation on either side of the river is Mojave Desert scrub, dominated by Joshua tree (*Yucca brevifolia*), creosote bush (*Larrea tridentata*), or white bursage (*Ambrosia dumosa*), all inhospitable for voles. Much of this region now is heavily impacted by urbanization, which has both encroached extensively on both banks of the Mojave River and is undoubtedly depleting the aquifer that nourishes the few patches of wetland habitat still supporting voles. Listed as a Species of Special Concern by the California Department of Fish and Wildlife.

Acknowledgments

We thank the curators at the Cleveland Museum of Natural History (T. Matson), Los Angeles Museum of Natural History (J. Dines), Museum of Zoology, University of Michigan (P. Myers and C. Edwards), and National Museum of Natural History (M. D. Carleton, A. L. Gardner, and S. Peurach) for access to, and for facilitating loans of, specimens from their respective institutions; and A. Gardner, E. Heske, R. Moratelli, and an anonymous reviewer for editorial and other suggestions that improved the text.

Supplementary Data

Supplementary data are available at *Journal of Mammalogy* online.

Supplementary Data SD1.—Specimens examined, including localities, geographic coordinates, and sample sizes.

Supplementary Data SD2.—Multivariate character comparisons for each character set for regional samples of *M. c. kernensis* and *M. c. vallicola*.

Supplementary Data SD3.—Scoring coefficients, eigenvalues, and % contribution for character set canonical variates analyses, principle components analyses, or multivariate correspondence analyses.

Supplementary Data SD4.—Pairwise *P*-values derived from Tukey–Kramer post hoc tests of each character set; classification matrices derived from canonical variates analyses; and contingency test results for character data set comparisons among the 5 subspecies samples of California voles.

Supplementary Data SD5.—Character set posterior probabilities of the a priori-defined subspecies groups *M. c. kernensis*, *M. c. vallicola*, and *M. c. scirpensis* and nonaligned population samples, with classification summaries for each character set and nonaligned sample.

Supplementary Data SD6.—Character set posterior probabilities of the a priori-defined subspecies groups *M. c. mohavensis*, *M. c. sanctdiegi*, and *M. c. scirpensis* and nonaligned population samples, with classification summaries for each character set and nonaligned sample.

Supplementary Data SD7.—Adjusted R^2 values and significance levels in comparisons of individual posterior probabilities of group membership derived from nuclear microsatellites and each of the 4 morphological character sets analyzed.

Literature Cited

Bailey, V. 1898. Descriptions of eleven new species and subspecies of voles. Proceedings of the Biological Society of Washington 12:85–90.

Bailey, V. 1900. Revision of American voles of the genus *Microtus*. North American Fauna 17:1–88 + 5 plates.

Berlin, B., D. E. Breedlove, and P. H. Raven. 1973. General principles of classification and nomenclature in folk biology. American Anthropologist 75:214–242

Berry, R. J., and A. G. Searle. 1963. Epigenetic polymorphism of the rodent skeleton. Proceedings of the Zoological Society of London 140:577–615.

Braby, M. F., R. Eastwood, and N. Murray. 2012. The subspecies concept in butterflies: has its application in taxonomy and conservation biology outlived its usefulness? Biological Journal of the Linnean Society 106:699–716.

Brenneman, R. A., et al. 2016. Genetic analysis of *Indri* reveals no evidence of distinct subspecies. International Journal of Primatology 37:460–477.

Conroy, C. J., and A. M. Gupta. 2011. Cranial morphology of the California vole (*Microtus californicus*, Cricetidae) in a contact zone. Biological Journal of the Linnean Society 104:264–283.

Conroy, C. J., and J. L. Neuwald. 2008. Phylogeographic study of the California vole, *Microtus californicus*. Journal of Mammalogy 89:755–767.

Conroy, C. J., J. L. Patton, M. C. W. Lim, M. A. Phuong, B. Parmenter, and S. Höhna. 2016. Following the rivers: historical reconstruction of California voles *Microtus californicus* (Rodentia: Cricetidae) in the deserts of eastern California. Biological Journal of the Linnean Society 119:80–98.

Grinnell, J. 1933. A review of the recent mammal fauna of California. University of California Publications in Zoology 40: 71–234.

Grinnell, J. 1935. Differentiation in pocket gophers of the *Thomomys bottae* group in California and southern Oregon. University of California Publications in Zoology 40:403–416.

Hall, E. R. 1981. The mammals of North America. 2nd ed. John Wiley & Sons, New York 2:601–1181.

Hammer, Ø, D. A. T. Harper, and P. D. Ryan. 2001. PAST: Paleontological Statistics Software Package for Education and Data Analysis. Palaeontologia Electronica 4:9 pp.

Hennig, W. 1966. Phylogenetic systematics. Translated by D. D. David and R. Zangerl. University of Illinois Press, Urbana.

Hill, G. E. 1998. An easy, inexpensive means to quantify plumage coloration. Journal of Field Ornithology 69:353–363.

Jombart, T., S. Devillard, and F. Balloux. 2010. Discriminant analysis of principal components: a new method for the analysis of genetically structured populations. BMC Genetics 11:94.

Kellogg, R. 1918. A revision of the *Microtus californicus* group of meadow mice. University of California Publications in Zoology 21:1–42.

Kellogg, R. 1922. Change of name. Proceedings of the Biological Society of Washington 35:78.

Lidicker, W. Z., Jr. 1962. The nature of subspecies boundaries in a desert rodent and its implications for subspecies taxonomy. Systematic Zoology 11:160–171.

Musser, G. M., and M. D. Carleton. 2005. Subfamily Muroidea. Pp. 894–1531 in Mammal species of the world: a taxonomic and geographic reference (D. E. Wilson and D. M. Reeder, eds.). 3rd ed. Johns Hopkins University Press, Baltimore, Maryland.

Remsen, J. V., Jr. 2010. Subspecies as a meaningful taxonomic rank in avian classification. Ornithological Monographs 67:62–78.

Sackett, L. C., et al. 2014. Evidence of two subspecies of Gunnison's prairie dogs (*Cynomys gunnisoni*), and the general importance of the subspecies concept. Biological Conservation 174:1–11.

Trujillo, A. L., and E. A. Hoffman. 2017. Uncovering discordance between taxonomy and evolutionary history in Florida raccoons. Systematics and Biodiversity 15:74–85.

Wilson, E. O., and W. J. Brown, Jr. 1953. The subspecies concept and its taxonomic application. Systematic Zoology 2:97–111.

Zink, R. M. 2004. The role of subspecies in obscuring avian biological diversity and misleading conservation policy. Proceedings of the Royal Society, Biological Sciences 271:561–564.

Submitted 7 March 2017. Accepted 25 May 2017.

Associate Editor was Ricardo Moratelli.